A&A 636, A107 (2020)
https://doi.org/10.1051/0004-6361/202037621

Astronomy & Astrophysics

Globular clusters in the Sagittarius stream

Revising members and candidates with *Gaia* DR2

M. Bellazzini[1], R. Ibata[2], K. Malhan[3], N. Martin[2,5], B. Famaey[2], and G. Thomas[4]

[1] INAF – Osservatorio di Astrofisica e Scienza dello Spazio di Bologna, Via Gobetti 93/3, 40129 Bologna, Italy
e-mail: michele.bellazzini@inaf.it
[2] Observatoire Astronomique, Université de Strasbourg, CNRS, 11, Rue de l'Université, 67000 Strasbourg, France
[3] The Oskar Klein Centre, Department of Physics, Stockholm University, AlbaNova 10691, Stockholm, Sweden
[4] NRC Herzberg Astronomy and Astrophysics, 5071 West Saanich Road, Victoria, BC V9E 2E7, Canada
[5] Max-Planck-Institut für Astronomie, Königstuhl 17, 69117 Heidelberg, Germany

Received 30 January 2020 / Accepted 17 March 2020

ABSTRACT

We reconsider the case for the association of Galactic globular clusters to the tidal stream of the Sagittarius dwarf spheroidal galaxy (Sgr dSph) using *Gaia* DR2 data. We used RR Lyrae variables to trace the stream in 6D and we selected clusters matching the observed stream in position and velocity. In addition to the clusters residing in the main body of the galaxy (M 54, Ter 8, Ter 7, Arp 2) we confirm the membership of Pal 12 and Whiting 1 to the portion of the trailing arm populated by stars lost during recent perigalactic passages. NGC 2419, NGC 5634, and NGC 4147 are very interesting candidates, possibly associated with more ancient wraps of the Sagittarius stream. With the exception of M 54, which lies within the stellar nucleus of the galaxy, we note that all these clusters are found in the trailing arm of the stream. The selected clusters are fully consistent with the [Fe/H] versus [Mg/Fe], [Ca/Fe] patterns and the age-metallicity relation displayed by field stars in the main body of Sgr dSph.

Key words. globular clusters: general – galaxies: individual: Sgr dSph – galaxies: dwarf – Galaxy: formation – Galaxy: stellar content

1. Introduction

The ongoing disruption of the Sagittarius dwarf spheroidal galaxy (Sgr dSph; Ibata 1994) provides a formidable case study of the ingestion of a dwarf satellite, which is a process that is generally considered a main driver of the formation of large galaxies (see e.g. Freeman & Bland-Hawthorn 2002, and references therein). Sgr dSph is populating the Milky Way halo with stars and presumably the dark matter particles that are lost along two huge tidal tails (Sgr stream). These tidal tails have been traced with various techniques over a huge range of distances (10−100 kpc; see e.g. Ibata et al. 2001; Newberg et al. 2002, 2007; Majewski et al. 2003; Belokurov et al. 2006; Niederste-Ostholt et al. 2010; Correnti et al. 2010; Belokurov et al. 2014, and references therein).

The Sgr dSph hosts four globular clusters (GCs) in its main body that were believed to belong to the GC system of the Milky Way (M 54, Arp 2, Ter 7, and Ter 8) before the discovery of the dwarf satellite. By analogy, additional Sgr GCs may have been lost in the disruption process and may lie immersed in the Sgr stream. Indeed the association of GCs to the Sgr stream was proposed long ago (Fusi Pecci et al. 1995; Irwin 1999; Palma et al. 2002) and then observationally supported (Bellazzini et al. 2003a; Law 2010a), at least on a statistical basis (see also e.g. Bellazzini et al. 2003b; Carraro et al. 2007; Paust et al. 2015; Carballo-Bello et al. 2017; Sollima et al. 2018, and references therein). In particular Law (2010a) discussed in detail the case for the membership or non-membership of new and previously proposed candidates, based on their correlation in 3D position and radial velocity with an *N*-body model of the disruption of the Sgr dSph (LM10 hereafter Law 2010b). Ten years later the LM10 model remains a reference model for the Sgr system.

The main limitation of these analyses was the lack of proper motions (PM) of sufficient precision (a) to test the full 3D motion of the stream and (b) to verify the coincidence of candidate GC members with stream stars in the 6D phase space. The exquisite astrometric precision achievable with the *Hubble* Space Telescope (Sohn et al. 2018) and, especially, with the second data release of the ESA/*Gaia* mission (*Gaia* DR2; Gaia Collaboration 2018a,b) has completely changed this scenario. Mean PM are now available for the majority of Galactic GCs with typical uncertainties $\leq$0.1 mas yr^{-1}, corresponding to $\leq$5.0(24.0) km s^{-1} for D = 10.0(50.0) kpc (Gaia Collaboration 2018b; Vasiliev 2019; Baumgardt et al. 2019). Direct detection and measurement of the 3D motion of Sgr stream stars can be obtained over the whole extension of the Galaxy (Hayes et al. 2020; Ibata et al. 2020, I20 hereafter).

Sohn et al. (2018) checked the membership of GCs in their sample by comparing with the prediction in the LM10 model in 6D. This model is known to provide a reasonably good description of the position and kinematics of the stars lost more recently by the Sgr galaxy, in particular up to three perigalactic passages before the present passage (Pcol $\leq$ 3; Hayes et al. 2020, I20)[1],

[1] The parameter Pcol is associated with each particle of the LM10 model, tagging the particles according to the perigalactic passage when they were stripped from the parent galaxy. The parameter Pcol = 0 is the current perigalactic passage, while Pcol = 1, 2,...,8 refers to one, two and up to eight perigalactic passages ago. Particles with Pcol = −1 are still gravitationally bound to the main body of the galaxy. The mean orbital period of the Sgr galaxy in the model is P = 0.93 Gyr (Law 2010b).

but it is unlikely to provide adequate predictions for more ancient arms of the Sgr stream, hence this technique of investigation is limited to the most recently lost clusters. The orbit of the progenitor of the Sgr system may have significantly evolved in the distant past (Belokurov et al. 2014), while the LM10 model adopts a static Galactic potential and does not include the effects of dynamical friction. In addition to the clusters in the main body, Sohn et al. (2018) indicates as likely members Pal 12 and NGC 2419 (see also Massari et al. 2017). In a search for clustering in the action-angle space, Vasiliev (2019) finds that Pal 12 and Whiting 1 (Carraro et al. 2007) are tightly grouped together with the main body clusters in that space. Massari et al. (2019), in an attempt to classify all the Galactic globulars according to their birth site using their orbital parameters, also propose Pal 12, Whiting 1, NGC 2419, and NGC 5824 as members of the Sgr system, in addition to the main body clusters. Just before the submission of this manuscript Antoja et al. (2020) presented a new analysis tracing the stream with *Gaia* PMs, detecting several possibly associated GCs. In addition to the four main-body clusters they explicitly confirm Pal 12 and NGC 2419 as members as well.

The approach adopted in this work is somewhat complementary to the analyses described above, and it is intended to provide a glance at the more ancient arms of the stream. The aim is not only to confirm candidates but also to find out the most promising, albeit still uncertain members, for further follow up. In particular, following I20, we trace the Sgr stream using RR Lyrae variables from *Gaia* DR2 (Clementini et al. 2019; Holl et al. 2018), and we look for clusters lying within and sharing the same space motion with the observed stream. We use the LM10 model only as a useful guideline for the interpretation of the observations (similar to Hayes et al. 2020, and I20).

All the magnitudes used in this paper have been corrected for interstellar extinction in the same way as described in I20, using reddening values obtained from the Schlegel et al. (1998) maps and recalibrated according to Schlafly & Finkbeiner (2011). The magnitudes of RR Ly used in this work are intensity-averaged mean magnitudes (Clementini et al. 2019). The PMs in equatorial coordinates, as extracted from the *Gaia* DR2 dataset, are denoted as `pmra` and `pmdec` (where `pmra` is already corrected for the $\cos(\delta)$ factor). In contrast with Law (2010a), who also considered the association of dwarf galaxies to the Sgr system, we limit our analysis to star clusters (see e.g. Longeard et al. 2020, for the possible association of the faint dwarf Sgr II).

2. Adopted samples

The I20 authors reported on the use of the `STREAMFINDER` code (Malhan & Ibata 2018; Malhan et al. 2018; Ibata et al. 2019) to trace the Sgr stream in the entire *Gaia* DR2 dataset (but limited to $G < 19.5$). The stream was detected at very high significance and its observed properties were used to define simple criteria aimed at selecting high-purity samples of stream stars. In particular, these criteria were used to select, from the `gaiadr2.vari_rrlyrae` catalogue (Clementini et al. 2019), a sample of stream RR Lyrae variables providing an independent validation of the `STREAMFINDER` distance scale. The distance to these RR Lyrae variables was computed using the M_G–[Fe/H] relation by Muraveva et al. (2018) and by adopting the mean metallicity of the subset with metallicity estimates from Fourier coefficients of their light curves (see Clementini et al. 2019); [Fe/H] = −1.3. We adopted the same distances in this work; in general we followed the same choices made in I20, if not otherwise stated. In the following we use the heliocentric Sagittarius coordinates $\Lambda_\odot$, $B_\odot$ as defined by Majewski et al. (2003) and revised by Koposov et al. (2012), where $\Lambda_\odot$ is the angle from the centre of Sgr along the orbital plane, with the leading arm of the stream at negative $\Lambda_\odot$ and the trailing arm at positive $\Lambda_\odot$, and $B_\odot$ is the angular distance in the direction perpendicular to the orbital plane.

We selected our RR Lyrae sample by tracing the Sgr stream adopting the following three of the four selection criteria adopted by I20:

1. $-20.0^\circ < B_\odot < +15.0^\circ$, i.e. stars near to the Sgr orbital plane
2. $-0.75\,\mathrm{mas\,yr^{-1}} < \mu_B + \mu_{B,\mathrm{reflex}} < 1.25\,\mathrm{mas\,yr^{-1}}$, where μ_B is the proper motion in the $B_\odot$ direction and adding $\mu_{B,\mathrm{reflex}}$ corrects for the reflex motion of the Sun in the same direction, to remove stars with large motions perpendicular to the orbital plane
3. $|\mu_\Lambda - mu_{\Lambda,\mathrm{fit}}| < 0.8\,\mathrm{mas\,yr^{-1}}$, where $mu_{\Lambda,\mathrm{fit}}$ is a polynomial tracing the mean PM of the stream as a function of $\Lambda_\odot$.

See I20 for the form and coefficients of the polynomial and for additional details and discussion on the above criteria. The 5385 RR Lyrae variables from the `gaiadr2.vari_rrlyrae` catalogue satisfying these conditions constitute our reference sample, which we name the Sagittarius Stream Selected Sample, hereafter 4S, for brevity. We dropped the fourth criterion by I20, which is similar to point 3 above, but concerns the mean motion in μ_B as a function of $\Lambda_\odot$, because, while it was useful to select the purest sample tracing the stars most recently lost from the Sgr dSph (within <3 Gyr), it turns out to be excessively restrictive for the present application. The adoption of this additional selection cut to the GCs sample leaves us with just the four main body clusters; however the membership of Pal 12 to the trailing arm, for instance, is confirmed by matching the orbit, detection of stream stars in the surroundings, and chemical tagging (see e.g. Sohn et al. 2018; Vasiliev 2019; Musella et al. 2018; Cohen 2004, and references therein). The set of criteria adopted in this work allowed us to trace very clearly the youngest stream arms while leaving open the possibility for the tentative detection of older structures. On the other hand, the adopted limits are convenient but somehow arbitrary and they can still be too restrictive to include all the present and past members of the Sgr system. Hence our census of clusters related to the stream may not be complete. To minimise the contamination from relatively nearby Galactic stars (especially from the bulge) that may creep in our selection window, we excluded all the stars having $D_\odot \leq 12.0$ Kpc.

In Fig. 1 we show the distribution of the 4S RR Ly in the heliocentric distance versus $\Lambda_\odot$ plane, and we compare this with the LM10 model, including PMs in the comparison[2]. The trailing arm is clearly seen to emerge from the main body (at $\Lambda_\odot = 0^\circ$ and $D_\odot \simeq 25$ kpc), is traced up to $\Lambda_\odot = +150^\circ$ and $D_\odot \simeq 35$ kpc, and has a relatively mild arching to $D_\odot \simeq 20$ kpc at $\Lambda_\odot = +80^\circ$. The discontinuities at $\Lambda_\odot \sim +60^\circ$ and $\Lambda_\odot \sim +120^\circ$ (as well as that around $\Lambda_\odot \sim -120^\circ$, in the leading arm) are artefacts due to incompleteness in the original catalogue, related to the scanning

[2] We multiplied the distances of the LM10 model by a factor of 0.94 to make the distance scale of the model more consistent with observations. This factor rescales the high value of the distance to the centre of Sgr dSph adopted in the LM10 model ($D_\odot = 28.0$ kpc) to a more generally accepted value ($D_\odot = 26.3$ kpc; after Monaco et al. 2004), in excellent agreement with the recent estimate obtained by Ferguson & Strigari (2019) using *Gaia* DR2 RR Lyrae.

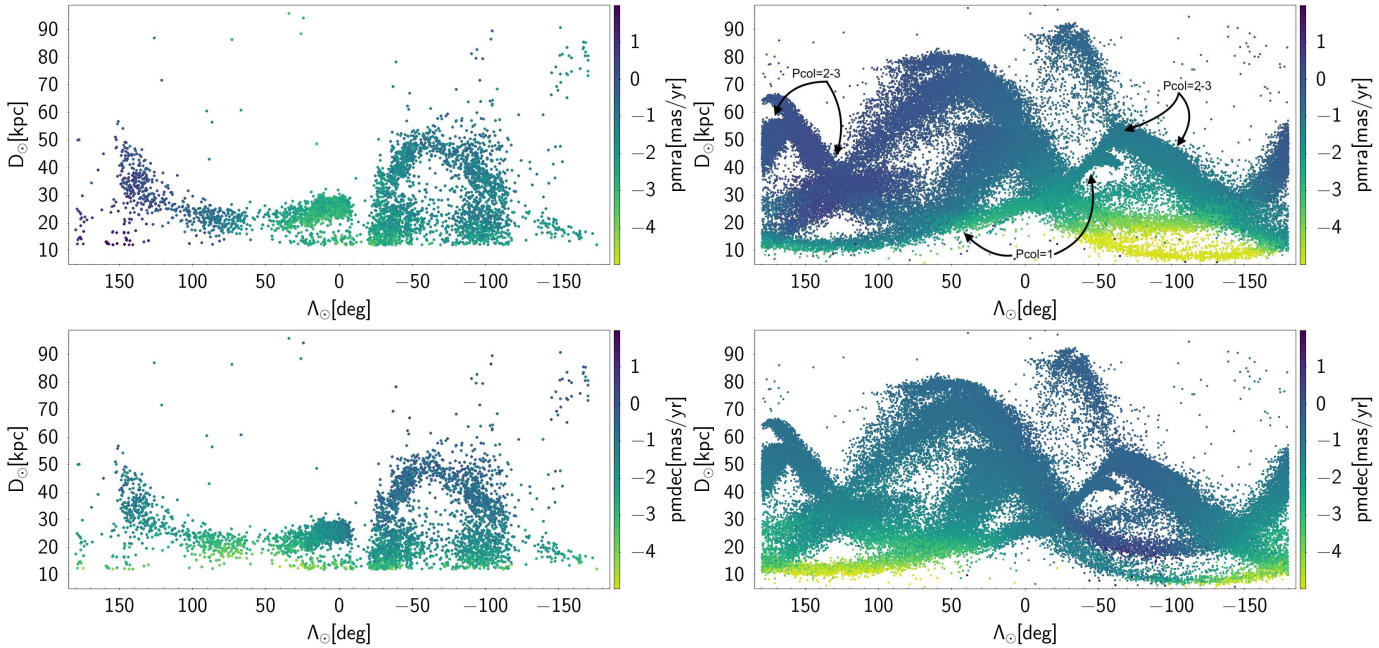

Fig. 1. Maps of the Sgr stream in the heliocentric distance vs. $\Lambda_\odot$ plane. *Left panels*: RR Lyrae variables from the DR2 4S. *Right panels*: particles of the LM10 model. Distances in the LM10 model are rescaled by a factor of 0.94 to make the embedded distance scale more consistent with observations. *Upper panels*: the points are colour coded according to their `pmra` values, in the *lower panels* according to their `pmdec`. *Upper right panel*: the approximate location of the transitions between portions of the stream dominated by Pcol = 0 (in the immediate surroundings of the main body), Pcol = 1, and Pcol = 2−3 particles (see also Fig. 5) are shown as reference.

law of *Gaia* (Clementini et al. 2019). The leading arm is seen to emerge from the Galactic disc at $\Lambda_\odot \simeq -30°$ and $D_\odot \simeq 30$ kpc, tipping at $\Lambda_\odot = -60°$ and $D_\odot \simeq 50$ kpc, and then declining more gently to $\Lambda_\odot = -180°$ and $D_\odot \simeq 15$ kpc. These are the most recent arms of the stream and are well matched by their counterparts in the LM10 model (also in radial velocity; see I20).

There are other features that are seen in the 4S sample and may have an identifiable counterpart in the LM10 model. First, the sparsely populated but clear arm at $-170° \lesssim \Lambda_\odot \lesssim -140°$ and 65 kpc $\lesssim D_\odot \lesssim$ 90 kpc, which encloses the cluster NGC 2419 (see below); this arm is likely the counterpart of the distant portion of the leading arm identified by Belokurov et al. (2014) with blue horizontal branch stars. The LM10 model has an handful of particles in that position, all of which have Pcol = 8, i.e. stripped during the most ancient perigalactic passage included in the model[3].

Second, according to the model, in the range $-100° \lesssim \Lambda_\odot \lesssim -50°$, four arms of the stream are crossed by the line of sight at $D_\odot \sim 10$ kpc (hence not included in the 4S), $D_\odot \sim 20$−25 kpc, $D_\odot \sim 35$ kpc, and finally the recent arm of the trailing arm described above, at $D_\odot \sim 50$ kpc. The sparse and old arms at 25 and 35 kpc have been confirmed observationally (see e.g. Correnti et al. 2010, and references therein) and seem to have a counterpart in the 4S sample as well, albeit the nearest arm has a significantly different mean PM with respect to the model predictions.

We applied the same selection criteria used to derive the 4S to the catalogue of GCs by Vasiliev (2019). This led to the selection of ten candidate members, namely, the four clusters in the main body plus Pal 12, Whiting 1, NGC 5634, NGC 4147, Pal 2, and NGC 6284. With the exception of the latter, all of these have been previously proposed as candidate members of the Sgr system (see e.g. Irwin 1999; Palma et al. 2002; Bellazzini et al. 2002, 2003a; Carraro et al. 2007; Law 2010a; Sohn et al. 2018; Vasiliev 2019, and references therein).

We added NGC 2419 to this selected sample because it is clearly immersed in (and has PM compatible with) the distant arm described above (see also Belokurov et al. 2014; Massari et al. 2017), although it does not pass all our selection criteria. The point is clearly illustrated in Fig. 2, where we zoom in on the stream arm near to the cluster. We consider the sample of RR Ly variables satisfying only the first two selection criteria represented above, as this sample traces the same structures but preserves a larger number of stars associated with the cluster. At $\Lambda_\odot = -170.1°$, corresponding to the position of the cluster, there is a tightly packed set of 22 RR Lyrae variables all aligned in the direction of the distance. This is the typical signature of a compact stellar system in this kind of diagram, especially at large distances. Other clusters display similar features and the Sculptor dSph is seen as a conspicuous vertical string, more extended than that associated with the typical GC. The blue dots in Fig. 2 are clearly RR Ly associated with NGC 2419. Their mean, reddening corrected G magnitude is $G_0 = 20.12$ with standard deviation $\sigma_{G_0} = 0.07$ mag. Using this mean magnitude and the appropriate metallicity for the cluster ([Fe/H] = −2.09; after Mucciarelli et al. 2012), the apparent mismatch in distance between the distant arm of the stream and the cluster is completely recovered. We note that four of the RR Ly associated with the cluster have metallicity estimates from Fourier coefficients, albeit with large errors. The resulting mean metallicity ($\pm 1\sigma$) is $\langle$[Fe/H]$\rangle = -2.07 \pm 0.60$, supporting the idea that they belong to a population more metal poor than the surrounding

[3] We note, however, that this specific match between the LM10 model and the 4S stars may be due to mere chance, as the predictions of the model for such ancient wraps of the stream are highly uncertain.

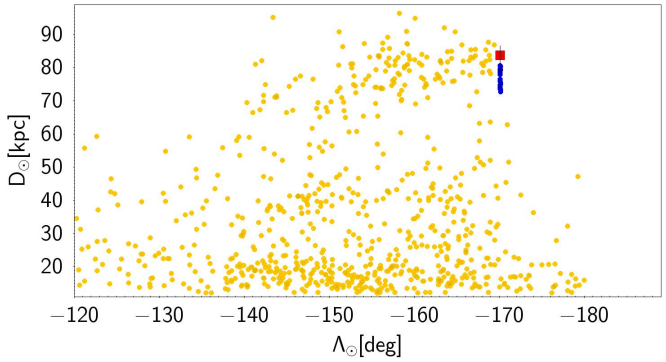

Fig. 2. Map of the *Gaia* RR Lyrae stars satisfying the selection criteria 1 and 2, zoomed in on the stream arm around the GC NGC 2419. The RR Lyrae variables belonging to the cluster are highlighted in blue. The red square indicates the mean distance of these RR Lyrae if the metallicity of the cluster is assumed ([Fe/H] = −2.09; after Mucciarelli et al. 2017), instead of the mean metallicity in the stream, [Fe/H] = −1.3.

stream; for the stars in Fig. 2 enclosed within $-170° < \Lambda_\odot \lesssim -150°$ and $70.0\,\mathrm{kpc} \leq D_\odot \leq 90\,\mathrm{kpc}$ we find $\langle[\mathrm{Fe/H}]\rangle = -1.40 \pm 0.66$ from 36 stars with metallicity estimates. Our final list of GCs candidate members of the Sgr system is shown in Table 1, where clusters are ranked according to the reliability of their association to the stream, according to the following analysis.

3. Star clusters in the Sgr stream

In Fig. 3 we compare the position of the selected clusters with the distribution of 4S RR Ly in the distance versus $\Lambda_\odot$ plane. It is important to note that the match between all the selected clusters and the stream arms in distance is not trivial, since none of the adopted selection criteria includes constraints on the distance (except for the case of NGC 2419). On the other hand, this match provides further support to the membership of these clusters to the Sgr system. Obviously not all the matches provide the same amount of support to membership, depending on the distance and/or the associations to portions of the stream that are more clearly characterised and successfully modelled.

In Fig. 4 we show that all the selected clusters have mean PMs in the range spanned by 4S RR Ly in the same range of distances, and there is a high degree of correlation. The only additional phase space parameter for which the match remains to be checked is the radial velocity. To do this last comparison we rely on the LM10 model. It has been demonstrated that this model provides a reasonable description of the radial velocity trend with $\Lambda_\odot$ for the most recent portions of both the leading and trailing arms (Hayes et al. 2020, I20). The radial velocity along more ancient arms is poorly known and, in these cases, LM10 at least provides a reference, albeit uncertain. To be homogeneous with the model we transformed the cluster heliocentric radial velocities into radial velocity in the galacto-centric reference frame (V_{GSR}) adopting the same solar motion adopted by LM10.

The comparison in V_{GSR} is presented in the lower panel of Fig. 5. In the upper panel of the same figure we plot the comparison in the usual distance versus $\Lambda_\odot$ plane, for reference. The LM10 particles are colour coded according to Pcol, thus providing a reference for the timescale of tidal stripping.

Table 1. Globular clusters matching position and PM of the Sgr dSph and stream as traced by *Gaia* DR2 4S RR Lyrae.

Name	Comment
	Members
NGC 6715 (M 54)	At the centre of the main body
Terzan 7	In the main body (Pcol = 0)
Arp 2	In the main body (Pcol = 0)
Terzan 8	In the main body (Pcol = 0)
Pal 12	In the trailing arm (Pcol = 0)
Whiting 1	In the trailing arm (Pcol = 1)
	Good/interesting candidate members
NGC 2419	Associated with a very distant and old arm (Pcol = 8)
NGC 5634	Possibly associated with an old arm (Pcol = 3−8)
NGC 4147	Possibly associated with an old arm (Pcol = 3−8)
	Unlikely candidate members
Pal 2	Compatible with an old arm (Pcol = 5−8) but >200 km s^{-1} difference in V_{GSR} with LM10
NGC 6284	Compatible with an old arm (Pcol = 4−8) but >250 km s^{-1} difference in V_{GSR} with LM10

Notes. The reported Pcol values indicate the Pcol range spanned by of the particles of the LM10 model in the surroundings of the cluster.

All the clusters also match, more or less closely, some branch of the stream in the V_{GSR} versus $\Lambda_\odot$ plane. However, in some cases, the match is only apparent, as the branch in which the clusters are immersed is not the same as that matched in velocity. An example that can be clearly identified in Fig. 5 is Pal 2, which is located within an ancient portion of the stream (Pcol = 5−8) and matches in V_{GSR} a recent branch (Pcol = 2−3), which is located at much larger distance. The LM10 model predicts $V_{\mathrm{GSR}} \simeq +120\,\mathrm{km\,s^{-1}}$ for the stream particles surrounding Pal 2, while the cluster has $V_{\mathrm{GSR}} = -107.1\,\mathrm{km\,s^{-1}}$. The case of NGC 6284 is even more extreme: the cluster is located in a branch at $V_{\mathrm{GSR}} \simeq -250\,\mathrm{km\,s^{-1}}$ while it has $V_{\mathrm{GSR}} = +32.5\,\mathrm{km\,s^{-1}}$. On the other hand, the branch in which NGC 4147 is immersed has a V_{GSR} that is more similar to that of the cluster. At the $\Lambda_\odot$ of the cluster this branch has a mean velocity of $V_{\mathrm{GSR}} \simeq +60\,\mathrm{km\,s^{-1}}$ but the overall velocity distribution reaches $V_{\mathrm{GSR}} \simeq +100\,\mathrm{km\,s^{-1}}$, while the cluster has $V_{\mathrm{GSR}} = +136.2\,\mathrm{km\,s^{-1}}$; this is a moderate mismatch. Similarly, NGC 5634 has $V_{\mathrm{GSR}} = -51.6\,\mathrm{km\,s^{-1}}$ and lies in the vicinity of an ancient portion of the stream with a mean $V_{\mathrm{GSR}} \simeq -100\,\mathrm{km\,s^{-1}}$, but reaches $V_{\mathrm{GSR}} \simeq -65\,\mathrm{km\,s^{-1}}$; this is a negligible difference, given the uncertainties. The radial velocity of NGC 2419, $V_{\mathrm{GSR}} = -27.1\,\mathrm{km\,s^{-1}}$ is within the range of the LM10 particles around the position of the cluster, $-57\,\mathrm{km\,s^{-1}} \lesssim V_{\mathrm{GSR}} \lesssim +62\,\mathrm{km\,s^{-1}}$.

All the other selected clusters match very well the radial velocity predicted by the LM10 model for the part of the Sgr system they are associated with. It is important to recall at this point that we can provide a safe confirmation only for clusters lying in the most recent wraps of the stream (Pcol $\lesssim 3$), where the radial velocity pattern predicted by LM10 broadly matches the observations. The predictions for more ancient wraps are more uncertain and must be considered with caution. As a consequence, the association of clusters with the old wraps are model dependent, at least concerning the radial component of the velocity. A spectroscopic follow up of candidate stream stars in the ancient

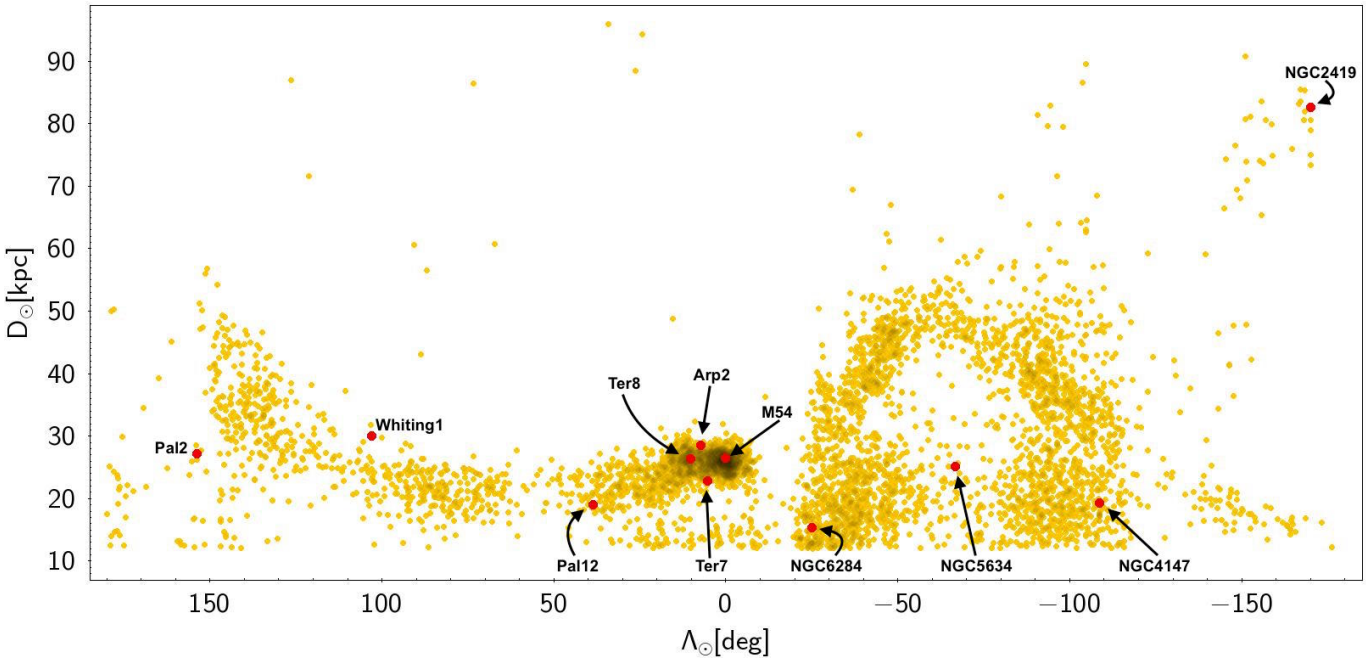

Fig. 3. Globular clusters selected as candidate members of the Sgr stream by their position and proper motion (red filled circles) are over-plotted on the map of RR Lyrae variables from the DR2 4S.

wraps is required for a final confirmation or rejection of these candidates.

3.1. Discussion on individual clusters

In the following we discuss the membership of each individual cluster in order of likelihood, based on the evidence presented in this analysis and in past literature.

3.1.1. Main body clusters

There has been little doubt of the membership of the four main body clusters since the very discovery of Sgr dSph (Ibata 1994; Da Costa & Armandroff 1995) owing to the coincidence in position and radial velocity with the galaxy. In particular, M 54 sits at the very centre of the galaxy within the stellar nucleus (Bellazzini et al. 2008; Alfaro-Cuello et al. 2019). Now their membership has also been fully confirmed with PMs (see e.g. Vasiliev 2019, and references therein).

3.1.2. Palomar 12

The cluster Pal 12 was first proposed as a possible member of the stream by Irwin (1999). Independent detection of stream stars in its surrounding were provided by Martinez-Delgado et al. (2002) and Bellazzini et al. (2003b). Cohen (2004) showed that its chemical composition is anomalous for a Galactic halo cluster but it is fully compatible with the abundance pattern observed in the Sgr galaxy (see e.g. Sbordone et al. 2015). Bellazzini et al. (2003a) and Law (2010a) proposed this cluster as a highly probable member of the stream, and Sohn et al. (2018), Vasiliev (2019) and Massari et al. (2019) confirmed these conclusions based on 6D space motion. In this paper we provide the additional support of the simultaneous 6D match with the observed stream, as traced by 4S RR Ly.

3.1.3. Whiting 1

The cluster was firstly proposed as a member by Carraro et al. (2007); this finding was confirmed by Law (2010a) and subsequently by Vasiliev (2019) and Massari et al. (2019). Its high metallicity and young age also support an extragalactic origin. We also confirm its membership to the young trailing arm.

3.1.4. NGC 2419

The massive and remote cluster NGC 2419 was suggested as possibly associated with the Sgr system as early as 20 years ago (Irwin 1999). The proximity with the orbital plane was also noted by Newberg et al. (2003), but Law (2010a) classified this cluster as unlikely to be a member. The possible connection with the stream, as traced by blue horizontal branch stars was noted by Ruhland et al. (2011). Sohn et al. (2018), Massari et al. (2017, 2019), based on space motion, strongly supported the membership of this cluster with the Sgr system. Belokurov et al. (2014) traced the stream out to the position of the cluster and also found a match in radial velocity. We fully confirm these conclusions: NGC 2419 is associated with the distant branch of the stream traced by 4S stars. Perhaps, it may still be possible that this branch is not associated with the Sgr Stream, but this seems quite unlikely.

3.1.5. NGC 5634

The cluster NGC 5634 was first proposed to be associated with an ancient wrap of the stream by Bellazzini et al. (2002, 2003a). Later Law (2010a) and Carretta et al. (2017) confirmed this cluster as a good candidate. In the metal-poor regime the abundance patterns of the Milky Way and of Sgr dSphs are very similar. Still Sbordone et al. (2015), based on detailed abundances of several elements in one cluster star, conclude that an origin in the Sgr system is more likely. A similar conclusion was reached also by

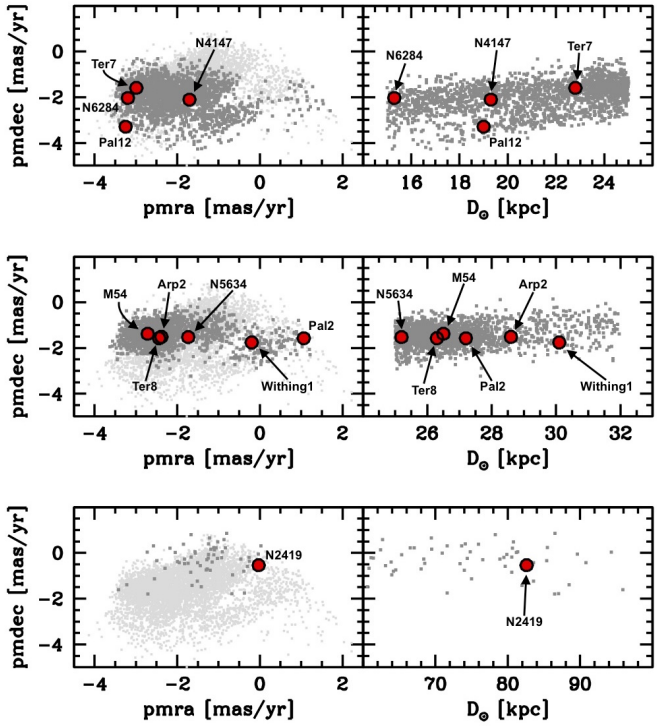

Fig. 4. Mean PM of candidate stream member GCs (red filled circles) are compared to the distribution of the 4S RR Lyrae variables (grey dots). The comparison is performed in the `pmdec` vs. `pmra` (*left panels*) and in the `pmdec` vs. heliocentric distance (*right panels*) planes in three different ranges of distance: $15.0\,\mathrm{kpc} < D_\odot < 25.0\,\mathrm{kpc}$ (*upper panels*), $25.0\,\mathrm{kpc} < D_\odot < 32.0\,\mathrm{kpc}$ (*middle panels*), and $60.0\,\mathrm{kpc} < D_\odot < 100.0\,\mathrm{kpc}$ (*lower panels*). The 4S RR Ly lying in the proper range of distance are plotted in dark grey, while the whole sample is plotted in pale grey in the *left-hand panels*.

Carretta et al. (2017) from an independent abundance analysis of a larger sample of cluster stars.

In this work we find that the cluster has a position and PM that is compatible with association with the ancient arm at $D_\odot \sim 20{-}25$ kpc already found by Correnti et al. (2010). It still needs to be checked observationally if the match extends to radial velocity. In this sense, the agreement with the LM10 model is not particularly meaningful since the model predicts a very different PM for this branch with respect to 4S RR Ly. However contamination by unrelated MW stars may be non-negligible in this region and the detection of this branch in the 4S must be confirmed with additional data (e.g. future data releases of *Gaia*, providing more complete samples of RR Lyrae variables). Taking all the above into account, we conclude that NGC 5634 remains a good candidate, to be confirmed with spectroscopic follow-up of the stream stars in its surroundings.

3.1.6. NGC 4147

The cluster was included in the list of possible candidates by Bellazzini et al. (2003a) and the stream was detected in its surroundings by Bellazzini et al. (2003b). Law (2010a) classified it as an attractive but weak candidate, while Sohn et al. (2018) rejects it based on the mismatch in PM with the LM10 model. If the 4S RR Ly variables in which the cluster is embedded are dominated by genuine members of the $D_\odot \sim 20{-}25$ kpc wrap of the stream, then NGC 4147 is an interesting candidate, and it is worthwhile to attempt a spectroscopic confirmation.

3.1.7. Palomar 2

The cluster Pal 2 was suggested as candidate member by Bellazzini et al. (2003b) and judged as a weak candidate by Law (2010a). The mismatch with the LM10 model is significant in all the three components of the velocity vector, however (as NGC 2419, NGC 5634, NGC 4147, and NGC 6284) the possible association is with an ancient wrap of the stream, where the predictions of the model lack observational verification. The match with the 4S stars around it is good.

3.1.8. NGC 6284

The cluster NGC 6284 was never suggested before as a possible member because of the careful cuts in galacto-centric distance adopted by both Bellazzini et al. (2003b) and Law (2010a) to avoid contamination by clusters near to the centre of the Galaxy, which are necessarily close to the orbital plane of Sgr. In principle, the case is analogous to Pal 2 but we consider it to be a more unlikely candidate as it may have been selected only because the distance cut adopted in this work was too liberal.

3.2. The distribution of clusters along the stream

According to Fig. 5, the clusters NGC 2419, NGC 5634, NGC 4147, Pal 2, and NGC 6284, if they are members, should have been lost by Sgr long ago, more than ∼3−5 Gyr ago. On the other hand, Pal 12 was lost during the current perigalactic passage and Whiting 1 was lost during the previous passage. It is interesting to note that the LM10 particles co-located, in phase space, with Arp 2, Ter 7, and Ter 8 became unbound during the current perigalactic, suggesting that also these "main body" clusters are being stripped. The density map of the main body shown in Fig. 6 shows that, indeed, they are all located in proximity of the apparent onset of the trailing tail, about $b \simeq -27°$, hence their ongoing stripping from the main body is not unlikely.

The position of these three clusters hints at an intriguing asymmetry in the distribution of GCs within the Sgr system: all the confirmed members (except for the nuclear cluster M 54) and the best candidates[4] are associated with the trailing arm and none with the leading arm of the stream. The initial ∼10° of the leading arm lies behind the densest part of the Galactic bulge and disc, where for example extreme interstellar extinction, in principle, may hide one or two unknown clusters. Nevertheless it is hard to imagine that clusters in the range $\Lambda_\odot \lesssim -20°$ may have escaped detection if they are similar to or brighter than Whiting 1 ($M_V = -2.55 \pm 0.44$, Muñoz et al. 2018), even taking into account that this part of the leading arm is more distant on average, than the trailing arm in the same range of Pcol. We note, however, that the two faint clusters Koposov 1 and Koposov 2 ($M_V = -1.04 \pm 0.69$, and $M_V = -0.92 \pm 0.81$, respectively; Muñoz et al. 2018) are not included in this analysis because they lack estimates of both PM and radial velocity, but are proposed as probable members of the stream based on their position (Paust et al. 2015) and both lie, in projection, on the leading arm. Also the cluster NGC 5824, proposed as a member of the system by Massari et al. (2019) would lie in the leading arm (at $\Lambda_\odot = -45.2°$, $D_\odot = 32.1$ kpc) but it is excluded from our selection by all the three adopted criteria. The study of the significance and of the possible origin of this asymmetry is beyond the scope of this paper, but the case is worth noting and may deserve further analysis.

[4] Those classified as "good/interesting" in Table 1.

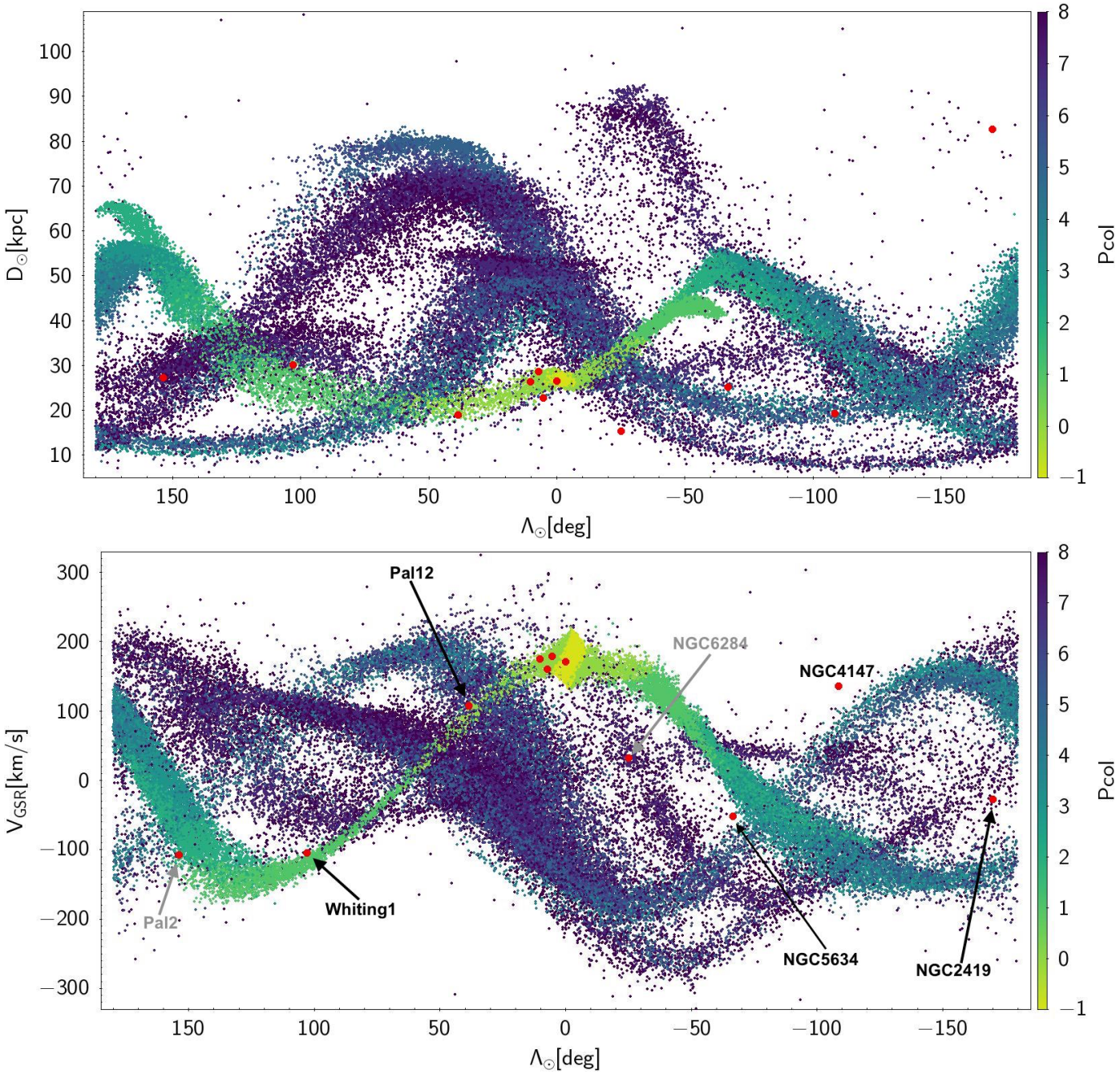

Fig. 5. Position (*upper panel*) and line of sight velocity in the Galactic standard of rest (V_{GSR}) of candidate stream member GCs (red filled circles) are compared to the predictions of the LM10 model. The model particles are colour coded according the perigalactic passage when they were stripped from the Sgr galaxy (Pcol). Pcol = 0 is the current perigalactic passage, while Pcol = 1,2,...,8 refers to one, two and up to eight perigalactic passages ago. Particles with Pcol = −1 are still gravitationally bound to the main body of the galaxy. Candidate clusters with V_{GSR} that is very different from the mean V_{GSR} of the stream arm they are immersed in are labelled in grey.

4. Summary and conclusions

We used the criteria developed by I20 to select a sample of Galactic GCs that lie within and have spatial motion compatible with the Sgr tidal stream, as traced by RR Lyrae variables in the *Gaia* DR2 catalogue. The membership of the clusters residing in the main body of the galaxy (M 54, Ter 8, Ter 7, Arp 2) and in the most recent wraps of the stream (Pal 12, Whiting 1) is confirmed beyond any reasonable doubt, while other candidates require additional observations and/or more refined modelling of the stream to be ultimately confirmed. NGC 2419, NGC 5634, and NGC 4147 may be immersed in more ancient wraps of the stream and they appear as particularly promising candidates.

Having considered all the available data to check the match in 6D phase space, the next step would be to look for consistency in the chemical composition and in the age-metallicity relation (see e.g. Carretta et al. 2017; Massari et al. 2019). While these factors already entered in the discussion of individual cases above, in Fig. 7 we attempt to provide a more global view of the α-elements versus iron chemical pattern and the age-metallicity relation of the clusters in comparison with the available data on field stars of Sgr dSph.

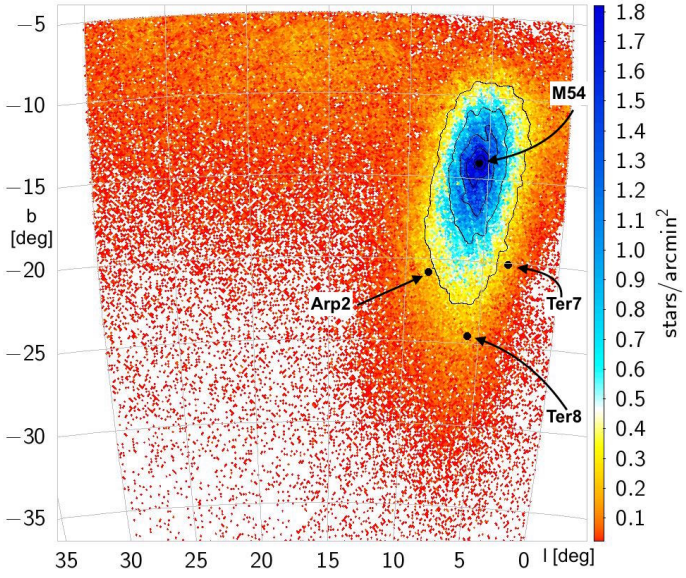

Fig. 6. Density map of the region at positive Galactic longitude around the Sgr galaxy, for *Gaia* DR2 stars that have PMs within 0.5 mas yr^{-1} from the mean PM of the galaxy (taken from Gaia Collaboration 2018b) and colours and magnitudes compatible with being members of the Sgr dSph. The clusters associated with the main body are indicated as filled black circles and are labelled.

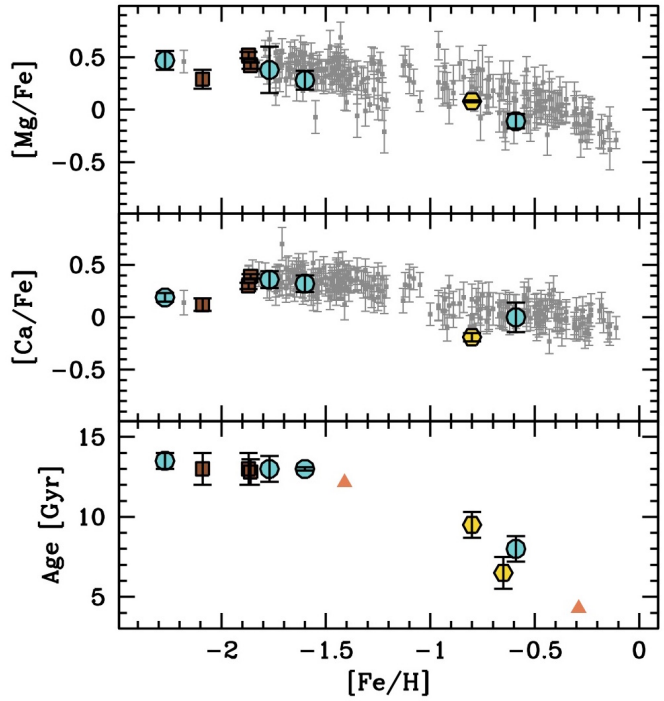

Fig. 7. [Mg/Fe] (*upper panel*) and [Ca/Fe] (*middle panel*) abundance ratios, and age as a function of [Fe/H] (*lower panel*) for main body clusters (turquoise filled circles), confirmed members (yellow filled hexagons), and good/interesting candidate members (brown filled squares), from Table 1. *Upper and middle panels*: we plotted field stars in the central region of Sgr dSph in gray (including M 54, from Mucciarelli et al. 2017); *lower panel*: we plotted, in orange triangles, the age and metallicity of the two main components of the Sgr field stars in the nuclear region (from Table 1 of Alfaro-Cuello et al. 2019), for comparison.

For the clusters, we take ages for all the clusters listed in this source from Dotter et al. (2010). The exception and the alternative sources are M 54 (Siegel et al. 2007), Whiting 1 (Carraro et al. 2007), and NGC 5634 (Bellazzini et al. 2002). For the chemical abundances we privileged the most recent studies based on high-resolution spectroscopy. In particular, we include M 54 (Carretta et al. 2010), Ter 7 (Sbordone et al. 2005), Ter 8 (Carretta et al. 2014), Pal 12 (Cohen 2004), NGC 5634 (Carretta et al. 2017), NGC 4147 (Villanova et al. 2016), and Whiting 1 (Carraro et al. 2007, no abundance ratio, only metallicity). For NGC 2419 we adopted the weighted mean of the individual abundances by Cohen et al. (2011), limited to the six stars of the Mg-rich population, i.e that reflecting the original composition of the cluster. In examining Fig. 7, it is important to bear in mind that non-negligible systematic differences between the abundance and age scales of these authors may affect the comparison between the various clusters as well as the comparision with the tracers of the field population included in the diagrams for reference (Mucciarelli et al. 2017; Alfaro-Cuello et al. 2019). Moreover, the field population is sampled only in the central region of the main body of the Sgr dSph, while the clusters (except M 54) populate/populated the outskirts.

With these caveats in mind, the result of Fig. 7, taken at face value, is that the consistency between the selected clusters and the field population of the Sgr dSph is excellent. In particular the field population of the Milky Way lies above the Sgr branch in the [Fe/H] versus [Mg/Fe], [Ca/Fe] diagrams for [Fe/H] > -1.0, hence in this regime the abundance of the clusters is discriminant and provides strong support to their membership to the Sgr system. It is also very intriguing that the only field star with [Fe/H] < -2.0 in Fig. 7 lies exactly between Ter 8 and NGC 2419, with very similar [Mg/Fe] and [Ca/Fe], at a value that does not match the extrapolation of the main branch of metal-poor stars to that metallicity. It is possible that a significant step in this context can be achieved when fully homogeneous ages and abundances are available for both the clusters and the field, and when the very metal-poor population of the galaxy is adequately sampled, while extending the comparison to more chemical elements (as done e.g. by Carretta et al. 2017, for NGC 5634).

Acknowledgements. MB acknowledges the financial support to this research by INAF, through the Mainstream Grant 1.05.01.86.22 assigned to the project "Chemo-dynamics of globular clusters: the *Gaia* revolution" (P.I. E. Pancino). RI, NM, BF and AS acknowledge funding from the Agence Nationale de la Recherche (ANR project ANR-18-CE31-0006, ANR-18-CE31-0017, and ANR-19-CE31-0017), from CNRS/INSU through the Programme National Galaxies et Cosmologie, and from the European Research Council (ERC) under the European Unions Horizon 2020 research and innovation programme (grant agreement No. 834148). We are grateful to G. Clementini and T. Muraveva for their advice on the RR Ly sample and to Denis Erkal and Antonio Sollima for useful discussions. This work has made use of data from the European Space Agency (ESA) mission *Gaia* (`http://www.cosmos.esa.int/gaia`), processed by the *Gaia* Data Processing and Analysis Consortium (DPAC, `http://www.cosmos.esa.int/web/gaia/dpac/consortium`). Funding for the DPAC has been provided by national institutions, in particular the institutions participating in the *Gaia* Multilateral Agreement. This research has made use of the SIMBAD database, operated at CDS, Strasbourg, France. This research has made use of the NASA/IPAC Extragalactic Database (NED) which is operated by the Jet Propulsion Laboratory, California Institute of Technology, under contract with the National Aeronautics and Space Administration. This research has made use of NASA's Astrophysics Data System.

References

Antoja, T., Ramos, P., Mateu, C., et al. 2020, A&A, 635, L3
Alfaro-Cuello, M., Kacharov, N., Neumayer, N., et al. 2019, ApJ, 886, 57
Baumgardt, H., Hilker, M., Sollima, A., & Bellini, A. 2019, MNRAS, 482, 5138
Bellazzini, M., Ferraro, F. R., & Ibata, R. 2002, AJ, 124, 915

Bellazzini, M., Ferraro, F. R., & Ibata, R. 2003a, AJ, 125, 188
Bellazzini, M., Ibata, R., Ferraro, F. R., & Testa, V. 2003b, A&A, 405, 577
Bellazzini, M., Ibata, R. A., Chapman, S. C., et al. 2008, AJ, 136, 1147
Belokurov, V., Zucker, D. B., Evans, N. W., et al. 2006, ApJ, 642, L137
Belokurov, V., Koposov, S. E., Evans, N. W., et al. 2014, MNRAS, 437, 116
Carballo-Bello, J. A., Corral-Santana, J. M., & Martínez-Delgado, D. 2017, MNRAS, 467, L91
Carraro, G., Zinn, R., & Moni Bidin, C. 2007, A&A, 466, 181
Carretta, E., Bragaglia, A., Gratton, R. G., et al. 2010, A&A, 520, A95
Carretta, E., Bragaglia, A., Gratton, R. G., et al. 2014, A&A, 561, A87
Carretta, E., Bragaglia, A., Lucatello, S., et al. 2017, A&A, 600, 118
Clementini, G., Ripepi, V., Molinaro, R., et al. 2019, A&A, 622, A60
Cohen, J. G. 2004, AJ, 127, 1545
Cohen, J. G., Huang, W., & Kirby, E. N. 2011, ApJ, 740, 60
Correnti, M., Bellazzini, M., Ibata, R. A., Ferraro, F. R., & Varghese, A. 2010, ApJ, 721, 329
Da Costa, G. S., & Armandroff, T. E. 1995, AJ, 109, 2533
Dotter, A., Sarajedini, A., Anderson, J., et al. 2010, ApJ, 708, 698
Ferguson, P. S., & Strigari, L. E. 2019, MNRAS, submitted [arXiv:1909.11103]
Freeman, K. C., & Bland-Hawthorn, J. 2002, ARA&A, 40, 487
Fusi Pecci, F., Bellazzini, M., Cacciari, C., & Ferraro, F. R. 1995, AJ, 110, 1664
Gaia Collaboration (Brown, A., et al.) 2018a, A&A, 616, A1
Gaia Collaboration (Helmi, A., et al.) 2018b, A&A, 616, A12
Hayes, C. R., Majewski, S. R., Hasselquist, S., et al. 2020, ApJ, 889, 63
Holl, B., Audard, M., Nienartowicz, K., et al. 2018, A&A, 618, A30
Ibata, R. A., Gilmore, G., & Irwin, M. J. 1994, Nature, 370, 194
Ibata, R. A., Irwin, M., Lewis, G. F., & Stolte, A. 2001, ApJ, 547, L133
Ibata, R. A., Malhan, K., & Martin, N. 2019, ApJ, 872, 152
Ibata, R. A., Bellazzini, M., Thomas, G., et al. 2020, ApJ, 491, L19
Irwin, M. J. 1999, IAU Symp., 192, 409
Koposov, S. E., Belokurov, V., Evans, N. W., et al. 2012, ApJ, 750, 80
Law, D. R., & Majewski, S. R. 2010a, ApJ, 718, 1128
Law, D. R., & Majewski, S. R. 2010b, ApJ, 714, 229
Longeard, N., Martin, N., Starkenburg, E., et al. 2020, MNRAS, 491, 356
Majewski, S. R., Skrutskie, M. F., Weinberg, M. D., & Ostheimer, J. C. 2003, ApJ, 599, 1082
Malhan, K., & Ibata, R. A. 2018, MNRAS, 477, 4063
Malhan, K., Ibata, R. A., & Martin, N. 2018, MNRAS, 481, 3442
Martinez-Delgado, D., Zinn, R., Carrera, R., & Gallart, C. 2002, ApJ, 573, L19
Massari, D., Posti, L., Helmi, A., Fiorentino, G., & Tolstoy, E. 2017, A&A, 598, L9
Massari, D., Koppelman, H. H., & Helmi, A. 2019, A&A, 630, L4
Monaco, L., Bellazzini, M., Ferraro, F. R., & Pancino, E. 2004, MNRAS, 353, 874
Mucciarelli, A., Bellazzini, M., Ibata, R., et al. 2012, MNRAS, 426, 2889
Mucciarelli, A., Bellazzini, M., Ibata, R., et al. 2017, A&A, 605, 46
Muñoz, R. R., Côté, P., Santana, F. A., et al. 2018, ApJ, 860, 66
Muraveva, T., Delgado, H. E., Clementini, G., Sarro, L. M., & Garofalo, A. 2018, MNRAS, 481, 1195
Newberg, H. J., Yanny, B., Rockosi, C., et al. 2002, ApJ, 569, 245
Musella, I., Di Criscienzo, M., Marconi, M., et al. 2018, MNRAS, 473, 3062
Newberg, H. J., Yanny, B., Grebel, E. K., et al. 2003, ApJ, 596, L191
Newberg, H. J., Yanny, B., Cole, N., et al. 2007, ApJ, 668, 221
Niederste-Ostholt, M., Belokurov, V., Evans, N. W., & Penarrubia, J. 2010, ApJ, 712, 516
Paust, N., Wilson, D., & van Belle, G. 2015, AJ, 148, 19
Palma, C., Majewski, S. R., & Johnston, K. V. 2002, ApJ, 564, 736
Ruhland, C., Bell, E. F., Rix, H.-W., & Xue, X.-X. 2011, ApJ, 731, 119
Sbordone, L., Bonifacio, P., Marconi, G., et al. 2005, A&A, 437, 905
Sbordone, L., Monaco, L., Moni Bidin, C., et al. 2015, A&A, 579, A104
Schlafly, E. F., & Finkbeiner, D. P. 2011, ApJ, 737, 103
Schlegel, D. J., Finkbeiner, D. P., & Davis, M. 1998, ApJ, 500, 525
Siegel, M. H., Dotter, A., Majewski, S. R., et al. 2007, ApJ, 667, L57
Sohn, S. T., Watkins, L., Fardal, M., et al. 2018, ApJ, 862, 52
Sollima, A., Martínez Delgado, D., Muñoz, R. R., et al. 2018, MNRAS, 476, 481
Vasiliev, E. 2019, MNRAS, 484, 2832
Villanova, S., Monaco, L., Moni Bidin, C., & Assman, P. 2016, MNRAS, 460, 2351